SCIENTIFIC PAPERS
OF THE UNIVERSITY OF PARDUBICE
Series A
Faculty of Chemical Technology
20 (2014)

STUDY OF COMPOSITIONAL CHANGES OF (Ag-)Sb-S THIN FILMS AFTER Ar^+ ION LASER IRRADIATION BY MEANS OF MICRO X-RAY FLUORESCENCE

Jan GUTWIRTH[1a], Petr BEZDIČKA[b], Tomáš WÁGNER[a]
and Miloslav FRUMAR[a]
[a]Department of General and Inorganic Chemistry,
The University of Pardubice, CZ–532 10 Pardubice,
[b]Institute of Inorganic Chemistry,
Academy of Sciences of the Czech Republic v.v.i.,CZ–250 68 Řež

Received March 31, 2014

Thin amorphous films from (Ag-)Sb-S system were prepared as potential candidates for new phase-change memory films. Amorphous (Ag-)Sb-S thin films were deposited by thermal evaporation (TE) of $Sb_{33}S_{67}$ bulk sample followed by optically induced diffusion and dissolution (OIDD) of thermally evaporated Ag thin films. The phase-change recording process was realized via photocrystallization experiments done by Ar^+ ion dot laser exposures of prepared films. Morphology of the laser exposed dots was observed by transmission optical microscopy while micro X-ray diffraction (μ-XRD) was utilized for determination of crystallinity of the exposed dots. Laser induced changes were quantified by

[1] To whom correspondence should be addressed.

local measurement of optical transmission in dependence on laser exposure time. Compositional changes are determined via micro-X-Ray Fluorescence (μ-XRF). The results prove crystallization of laser exposed thin film. Kinetic of this process is described in terms of transmittance change, evolution of X-Ray diffractograms and changes observable by optical microscopy. Moreover, the results do not indicate any significant chemical change in the case of stoichiometric Sb_2S_3 *after laser irradiation while certain migration of silver takes place in sulfur rich Sb-S films doped by Ag.*

Introduction

Non volatile rewritable data storage is one of the recent applications of chalcogenide thin films [1-4]. Generally, there are two phenomena utilized for non volatile rewritable data storage based on chalcogenide thin films. The first one is reversible phase change between amorphous and crystalline state and *vice versa* used in commercially available rewritable optical discs (such as well known CD, DVD, HD-DVD or Blu-ray Discs) [5,6] or electrically switched chalcogenide phase change memories (denoted as Ovonic Unified Memory (OUM) or Phase Change Random Access Memory/Chalcogenide Random Access Memory (PC-RAM, P-RAM, C-RAM)) [2,7,8]. The second phenomenon is electrically induced reversible dissolution and separation of metallic Ag and *vice versa* in the system of Ag doped chalcogenide glass, denoted as Programmable Metallization Cell (PMC) Memory [9-11].

Principally, phase changes are caused by laser or electrical pulses with different power and duration. The detection consists in reflectivity difference (optical memories) or electrical resistance difference (PC-RAM) of amorphous and crystalline state in the case of phase change memories. Whereas, Ag dissolution in chalcogenide matrix or Ag separation from silver doped chalcogenide glass takes place due to migration of Ag^+ ions caused by DC electrical pulses in programmable metallization cells. The detection is based on different electrical resistance of undoped and Ag doped chalcogenide glass.

There are some elementary considerations for material feasibility for phase change recording. These basic considerations [5] are namely on thermal and optical or electrical properties due to photo-thermal or electro-thermal origin of phase transformation as well as optical or electrical based detection, respectively. Also some properties given by practical application are requested as well.

Sufficient reflectivity contrast between amorphous and crystalline phase for detection wavelength is necessary for high Signal to Noise Ratio (SNR) which allows high speed or multilevel data storage [5,12]. Also, sufficient absorption of both phases for writing/erasing wavelength is necessary for data recording realization. Requirements for thermal properties of recording materials are given

by disc stability and stability against self crystallization during storage or during writing/erasing of neighbour data domains, respectively. Due to the first requirement, tendency to minimize melting point T_m (typically ~ 600 °C) occurs. On the other hand, due to the second requirement, the crystallization temperature T_c or even the glass transition temperature T_g must be over 100 °C. Good stability of amorphous and crystalline phase against separation during recording processes or storage is also required for achieving good cyclability (high reversibility of phase transformation) of material as well as high crystallization rate [5].

Widely used active recording films materials are based on doped Sb-Te alloys [2,6,12,13]. Mostly used materials are from Ge-Sb-Te (GST) [14,15] and Ag-In-Sb-Te (AIST) [16,17] system.

Density Functional Theory (DFT) calculations carried out on chalcogenide materials of $AgSbCh_2$ compound [18], where Ch is S, Se or Te, suggest them to be promising materials for application as the active recording films.

Hence, there is sufficient research effort concerned about improvement current materials and research and development of new ones. Commercially used materials as GST or AIST are studied intensively due to elucidation of phase change principle at nanoscale [4,18-25] or materials improving [26-28], while new materials, e.g., from system Ag-Sb-Ch [18] where Ch is S [29-32] or Se [33-36] or Te [37-39]) are studied mainly in terms of thermal, optical and electrical properties and their engineering towards data storage application.

There are several papers dealing with laser interaction with Sb_2Ch_3 (Ch = S, Se, Te) thin films, e.g., Refs [40-43], which conclude that the optical contrast between unexposed and laser exposed dots is connected with large change of chemical composition.

The aim of this work is to prove origin of optical contrast observed after laser irradiation of (Ag-)Sb-S thin films and describe the crystallization process.

Materials and Methods

Starting $Sb_{33}S_{67}$ bulk sample was synthesized in an evacuated silica glass ampoule from elements of 5N purity in electric rocking furnace S02 (Vezas, the Czech Republic). Preliminary synthesis pressure was $p \sim 10^{-3}$ Pa, synthesis temperature was $T \sim 750$ °C during time of $t = 24$ hours. Polycrystalline bulk was obtained by cooling of the ampoule with the melt in water ($T \sim 10$ °C).

Prepared bulk was used as a source for thermal evaporation (TE) of Sb-S thin films. Thermal evaporator UP 858 (Tesla, the Czech Republic) pumped down by a diffusion and rotary vane pump was used for the depositions. Pressure was monitored through a hot cathode gauge of Bayard Alpert type. Thickness homogeneity was guaranteed by planetary rotation of substrates (microscope slides). Deposition rate as well as thickness of deposited thin film was monitored

via quartz crystal monitor (QCM) MFV1843/A (Miky FFV/Miky Pulley, Japan). Background pressure was $p \sim 10^{-4}$ Pa and the deposition rates were 2 nm s^{-1} and 10nm s^{-1}. Silver doping was done by optically induced diffusion and dissolution (OIDD) [44,45] of Ag. Silver thin films were thermally evaporated on top of the Sb-S host matrixes. TE of Ag was carried out directly from molybdenum boat in the same system, at preliminary pressure $p \sim 10^{-4}$ Pa and deposition rate ~ 0.3 nm s^{-1}. Resulting bilayer system was illuminated from chalcogenide glass side by a tungsten lamp focused by large Fresnel lens with IR cut-off filter ($I \sim 80$ mW cm^{-2}). This process results in homogeneous amorphous (Ag-)Sb-S thin films.

Thicknesses of all the thin films have been confirmed by Swanepoel technique [46] and vary close to 750 nm [30,31].

Composition and homogeneity of prepared bulk was checked by SEM-EDX technique provided by a microscope JSM – 5500 LV (Jeol, Japan) equipped with energy dispersion analyser (IXRF Systems, USA) and Si(Li) detector Sirius 10 (Gresham, e2v Scientific Instruments, UK). Applied accelerating voltage was $U = 20$ kV. Ag-L, Sb-L and S-K lines were used for analysis.

Possibility of application as an active material for rewritable optical data storage was tested *via* dot laser exposures. Dot laser exposures were carried out by an Ar^+ ion laser ($\lambda = 514.5$ nm) Innova 300C model I-304 (Coherent, USA) of output power $P = 845.5$ mW and beam diameter $d = 1.1$ mm (i.e., intensity $I = 89$ W cm^{-2}). Exposure time was scaled from 1 s to 20 s.

Dot laser exposures were characterized by several techniques, i.e., by transmission optical microscopy, micro X-ray diffraction (μ-XRD) and by measurement of photocrystallization kinetic curves (i.e., measurement of optical transmission in dependence on laser exposure time).

Transmission optical microscopy was realized *via* a standard microscope Carl Zeiss Jena (Zeiss, Germany) equipped with a digital camera Coolpix 990 (Nikon, Japan).

Micro-XRD was measured by diffractometer X'PertPRO (PANalytical, The Netherlands) with Co Kα X-ray tube ($U = 30$ kV, $I = 45$ mA) and Fe β filter. Silica monocapillary (diameter $d = 0.1$ mm) was used as a primary optics while secondary optics was Soller slits (0.04 rad). Multichannel semiconductor detector X'celerator (PANalytical, The Netherlands) with anti-scatter shield was used for detection. Qualitative analysis was performed with HighScore software package, version 1.0d (PANalytical, The Netherlands), Diffrac-Plus software package, version 8.0 (Bruker AXS, Germany) and JCPDS PDF-2 database [47].

Photocrystallization kinetic curves (dependence of optical transmission on laser exposure time) were collected by a Schnellphotometer (Zeiss, Germany) with photomultiplier and optical system Opton. Polychromatic light with circular beam of diameter $d = 120$ mm was used for measurement.

Compositional deviations of laser exposed dots were determined by mapping option of micro-X-Ray Fluorescence (μ-XRF). Spectrometer EAGLE II

(Röntgenanalytik Meßtechnik GmbH, Germany) equipped with Energy-Dispersive X-Ray (EDX) analyser was utilized. Sample was excited by Rh X-Ray tube when accelerating voltage of 40 kV and current of 400 μA was applied. Excitation radiation was focused through silica polycapillary optics to spot with a diameter of 50 μm. Radiation outcoming from sample was detected by an Si(Li) detector EAGLE 149-5 (EDAX International, USA). Detector signal was analyzed *via* a multichannel analyser EDAM3 BOX (EDAX International, USA). Analysis was performed in vacuum ambient when Ag-L, Sb-L and S-K lines were used for analysis of of 32×25 point (covering area 1.6×1.0 mm) matrix.

Results and Discussion

Chemical compositions of deposited thin films are summarized in Table I. Both Sb-S host matrixes are sulfur depleted in comparison to the source bulk sample. The depletion is more significant for deposition rate of 2 nm s^{-1} when the composition of thin films is very close to stoichiometric Sb_2S_3.

All the thicknesses of the prepared thin films (Table I) are close to 750 nm [30,31] which fact guarantes significant absorption of laser used for exposures.

Table I Composition of prepared thin films as determined by SEM-EDX and thickness of prepared thin films [30,31]

Sample	OIDD Ag, nm		Composition, % at.			Film thickness nm
	Number of steps	Total thickness nm	Ag	Sb	S	
b2-0	0	0	0	39.7	60.3	721.7
b2-5	1	5	1.1	39.1	59.8	730.0
b2-10	2	10	2.4	38.4	59.2	744.3
b10-0	0	0	0	36.7	63.3	805.3
b10-20	2	20	4	35.3	60.7	761.0
b10-47	1	47	8.5	32.4	59.1	770.4

Observation of dot laser exposures (Fig. 1.) by bright field transmission optical microscopy shows dark spots, i.e., laser irradiation causes changes resulting to decreasing of optical transmittance. Area of these spots increases with increasing exposure time. Dots are homogeneous with sharp edges in the case of

Ag free samples. Silver addition leads in the case of longer exposure times to creation of ring-shape halo which is relatively narrow and poorly visible for all the samples except sample b10-47 where the halo is broad and clearly visible. Deeper study reveals formations of cracks or even peeling off thin film in case of Ag doped b10 samples.

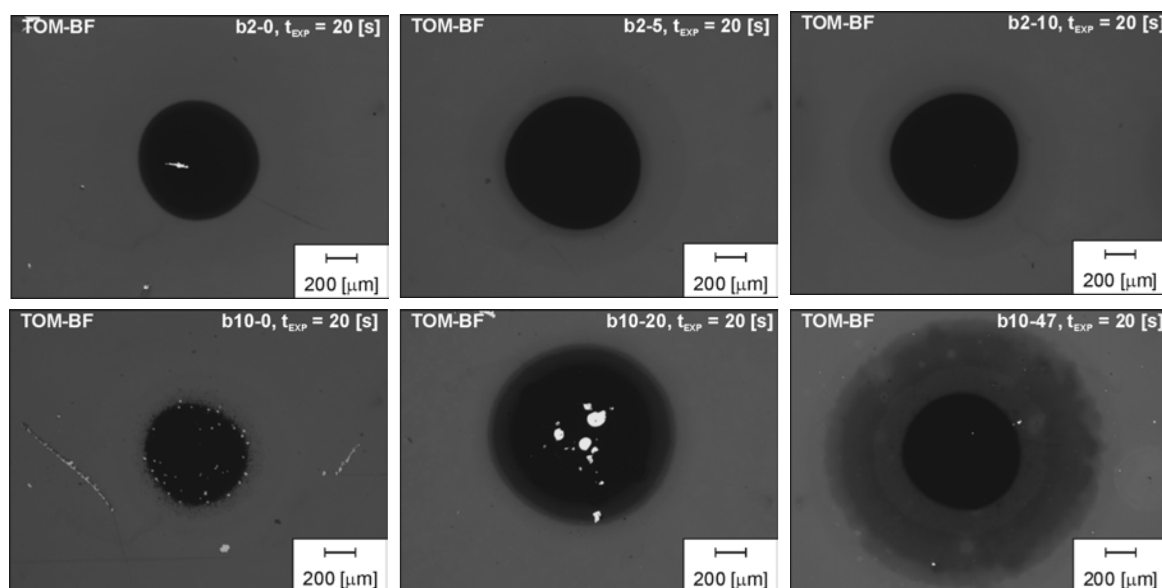

Fig. 1 Transmission optical microscopy images of laser exposed dots (exposure time t_{EXP} = 20 s) on particular thin films

Laser caused changes are quantified *via* photocrystallization kinetic curves as depicted in Fig. 2. Several significant differences are visible. The total time of crystallization (given as ~ 0 % optical transmittance) is shorter for b2-0 sample (t_{EXP} = 8 s) in comparison with b10-0 sample (t_{EXP} = 10 s). Addition of silver does not influence the total time of crystallization in the case of b2 samples in contrast to b10 samples, where the total time of crystallization is strongly reduced by silver addition. The shape of photocrystallization kinetic curves is rather complicated in the case of b2 samples while in the case of b10 samples the shapes of the photocrystallization kinetic curves are close to sigmoidal shape. Exception is b10-47 sample where two steps are clearly visible.

Laser exposed dots are studied by X-Ray diffraction. All the samples contain orthorhombic Sb_2S_3. Ag doped samples moreover contain rhombohedral Ag_3SbS_3 in the case of b2 samples and cubic $AgSbS_2$ in the case of b10 samples, respectively [30,31]. In the case of b10-47 sample, where two abrupt changes are visible within the photocrystallzation kinetic curve, XRD of all the exposed dots was measured as presented in Fig. 3. From these measurements results that the crystallization takes place in two steps. The first step (t_{EXP} = 1-3 s) corresponding to crystallization of cubic $AgSbS_2$ while the second step (t_{EXP} = 7-8 s) corresponding to crystallization of orthorhombic Sb_2S_3. This result also

corresponds with transmission optical microscopy observation, where dark central part of exposed dots arises at t_{EXP} = 8 s. Thus, it can be considered that while central dot contains cubic $AgSbS_2$ and orthorhombic Sb_2S_3, the halo contains cubic $AgSbS_2$ and Ag depleted amorphous matter.

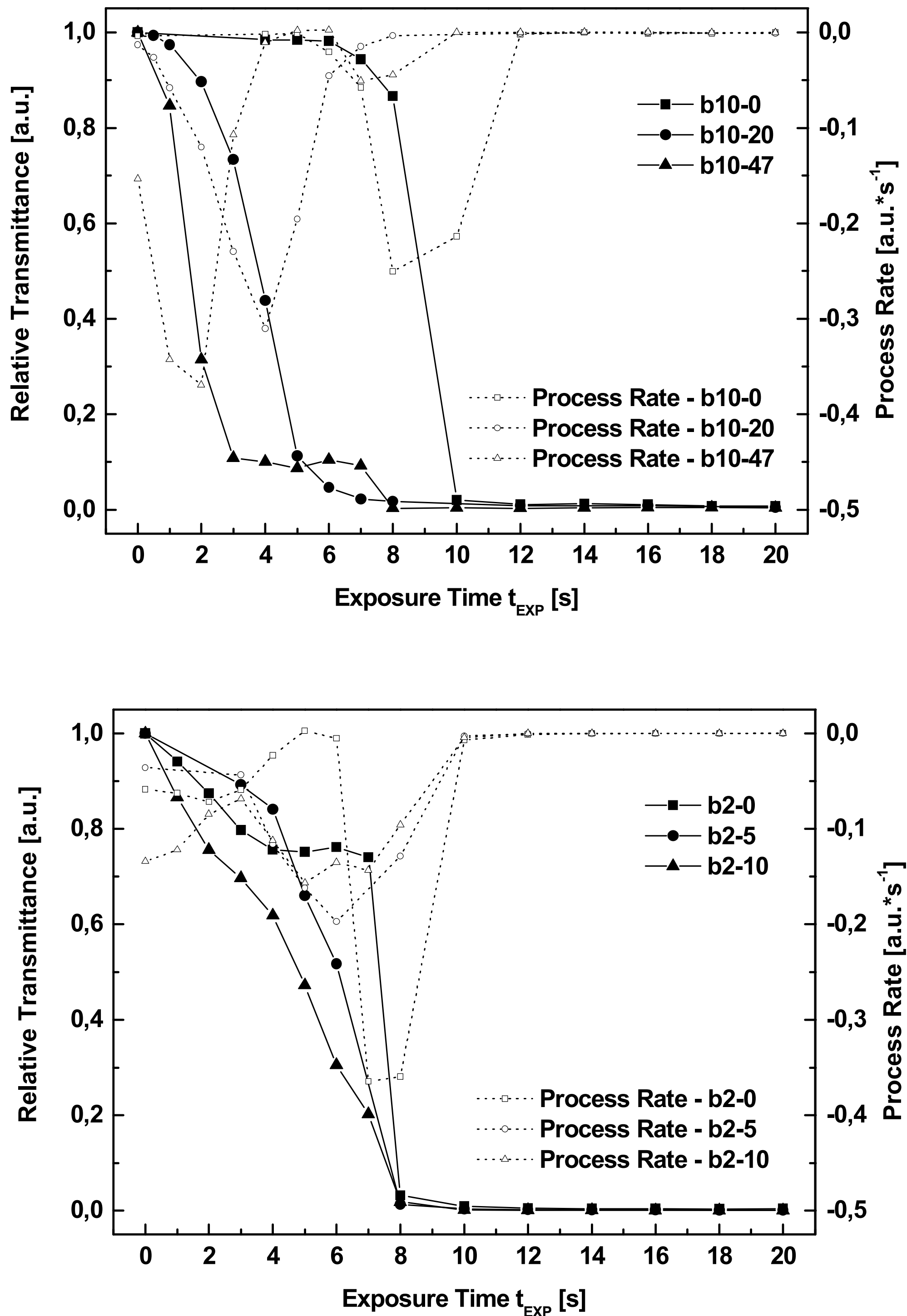

Fig. 2 Photocrystallization kinetic curves; dependence of optical transmittance on laser exposure time together with numerically derived signal

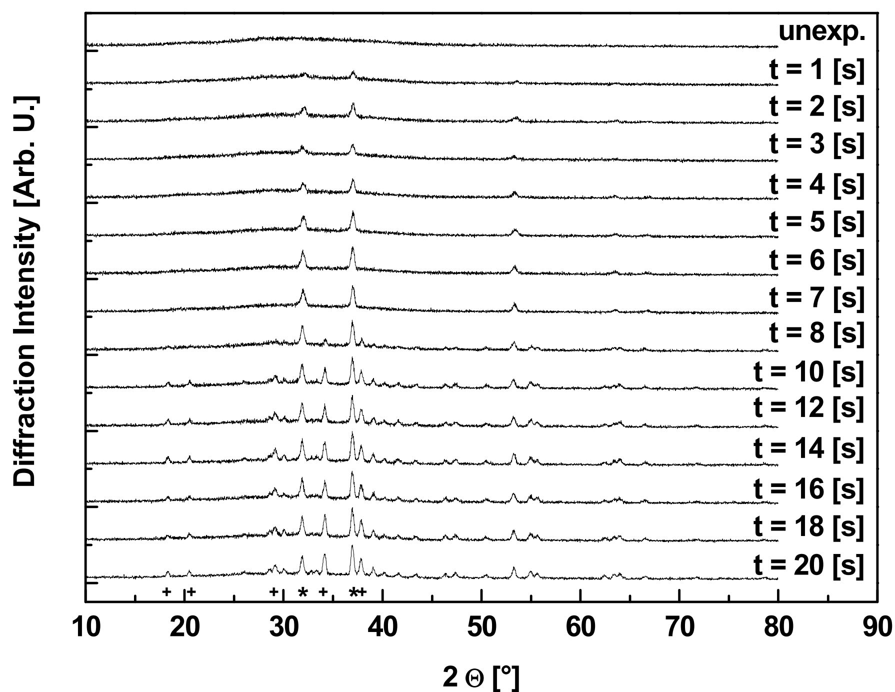

Fig. 3 X-Ray diffractograms of b10-47 sample for different exposure times. Diffraction lines are attributed as follows: + – orthorhombic Sb_2S_3, * – cubic $AgSbS_2$

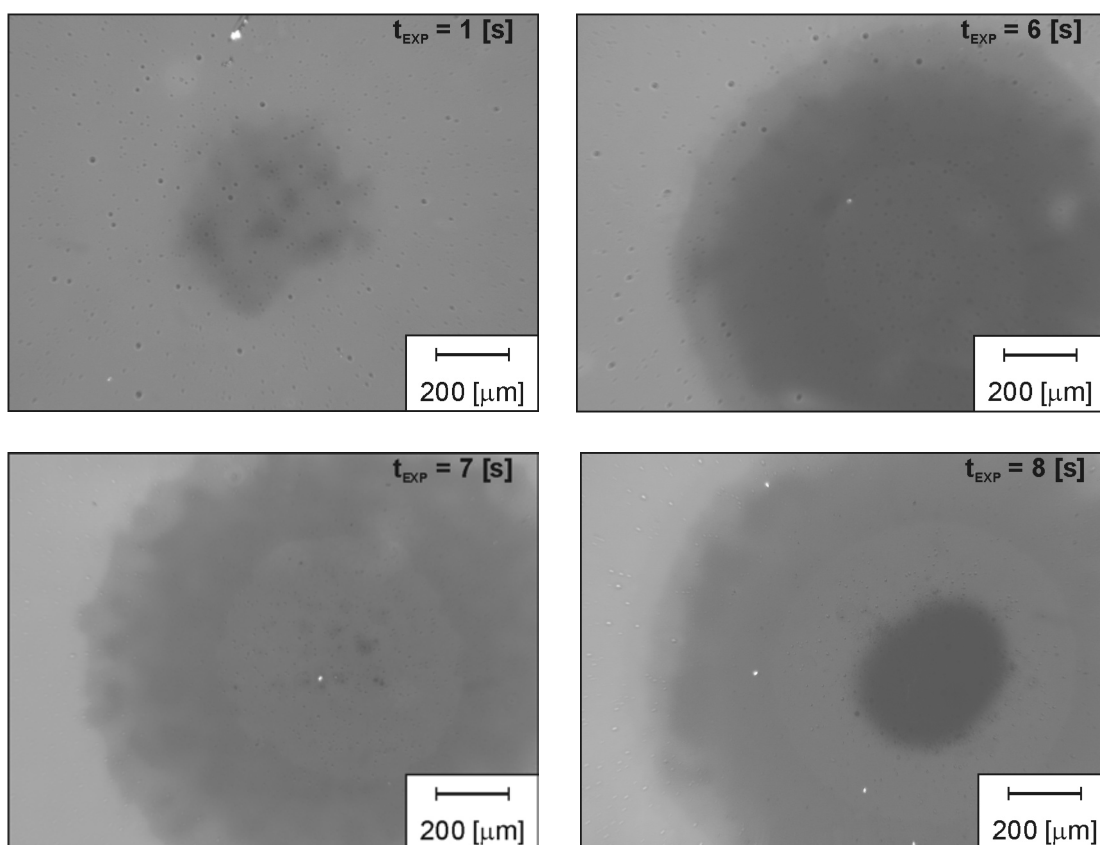

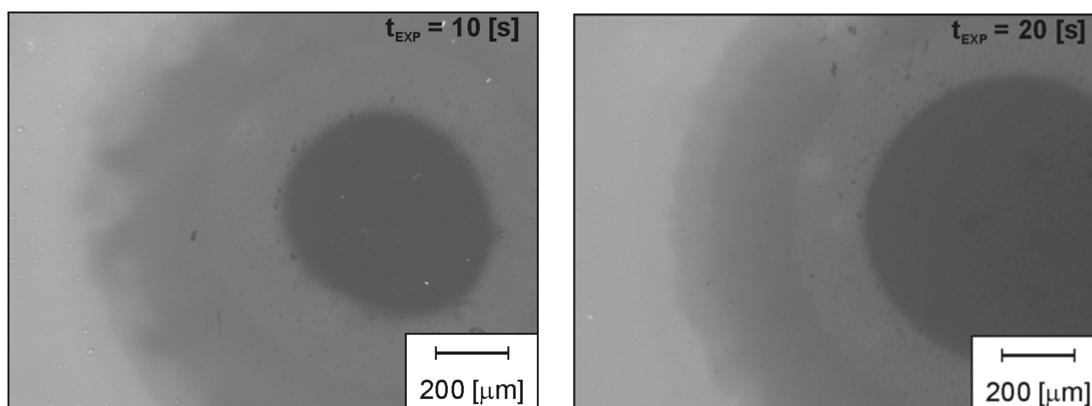

Fig. 4 Transmission optical microscopy images of laser exposed dots with different exposure times on b10-47 sample

Results of XRF study of laser exposed dots (t_{EXP} = 20 s) are presented in Figs 5 and 6 for samples b2-0 and b10-47. There are no compositional changes observed in the case of b2-0 sample in contrast to Refs [40,43]. However, in the case of b10-47 sample, a mild (ca 3 % at.) silver enrichment was detected in border between halo (i.e., cubic $AgSbS_2$ and amorphous Ag depleted Ag-Sb-S matrix) and unexposed film (i.e., amorphous $Ag_{8,5}Sb_{32,4}S_{59,1}$).

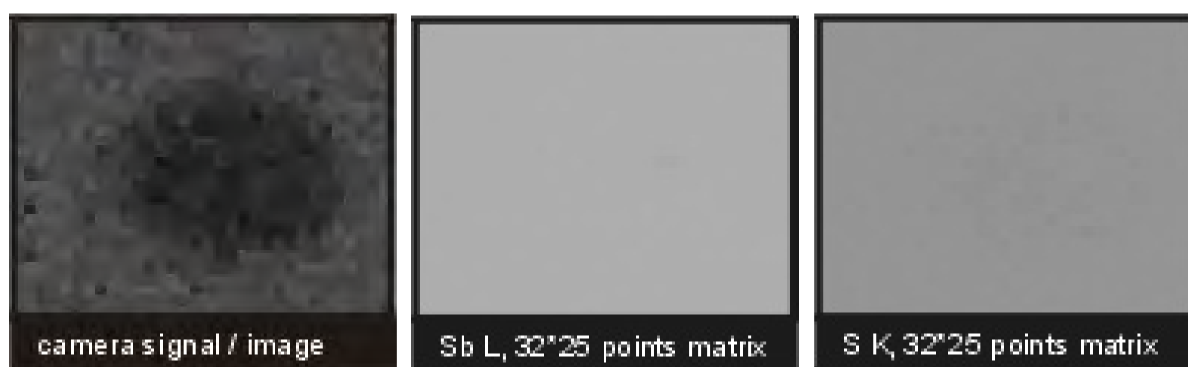

Fig. 5 XRF compositional maps together with image of analyzed laser exposed dot (t_{EXP} = 20 s) of b2-0 sample

Conclusion

Thin amorphous films of (Ag-)Sb-S ternary system were successfully prepared by thermal evaporation of host Sb-S matrix followed by optically induced diffusion and dissolution of silver. Laser exposures cause crystallization of thin films. The influence of Sb-S stoichiometry and Ag concentration to crystallization behaviour is described.

In contrary to previously published works, there is no significant change in the chemical composition observed in the case of stoichiometric Sb_2S_3 thin films.

Only in the case of silver doped sulfur rich thin films undergoing two-step crystallization process, silver migration is observed after laser irradiation.

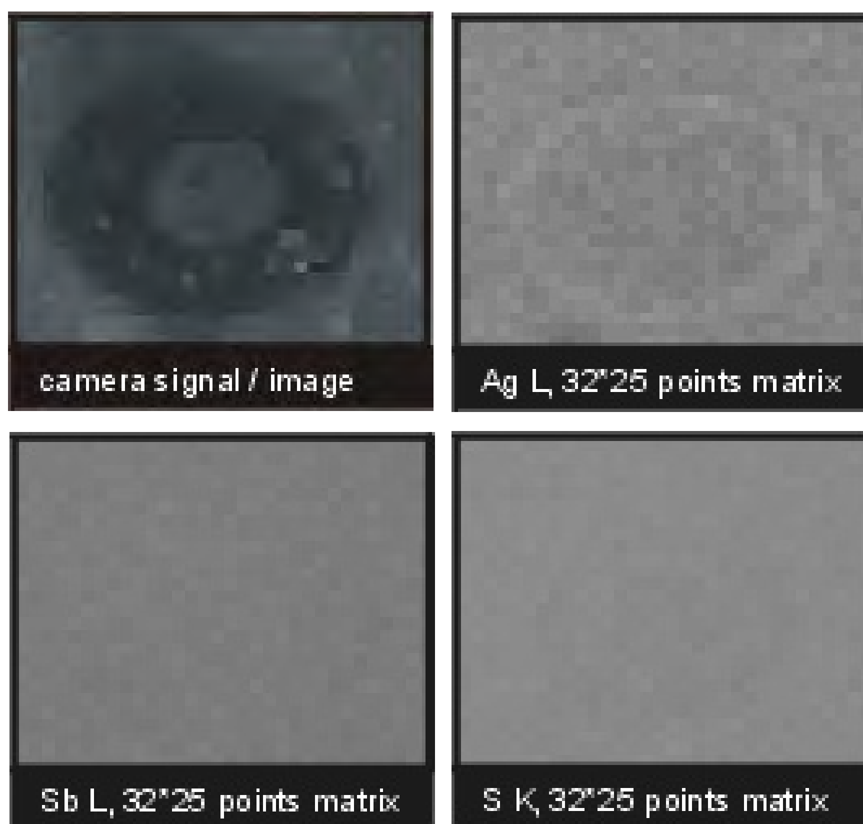

Fig. 6 XRF compositional maps together with image of analyzed laser exposed dot (t_{EXP} = 20 s) of b10-47 sample

Acknowledgment

The authors thank to grant projects CZ.1.07/2.3.00/30.0021 "Strengthening of Research and Development Teams at the University of Pardubice" and CZ.1.07/2.3.00/09.0104 "Education and Development of Research Team for Centre of Material Science Pardubice" realized by European Social Fund and the Ministry of Education, Youth and Sports of The Czech Republic within The Education for Competitiveness Operational Programme for financial support. The authors also thank to Dr. Milan Vlček (Joint Laboratory of Solid State Chemistry of University of Pardubice and Institute of Macromolecular Chemistry AS CR v.v.i.) for SEM-EDX measurements.

References

[1] Milster T.D. in: *The Optics Encyclopedia – Basic Fundations and Practical Applications*, Vol. 1 (Brown Th.G., Creath K., Kogelnik H., Kriss M.A., Schmit J., Weber M.J., Eds.), pp 227-274, Wiley-VCH, Weinheim, 2004.
[2] Wuttig M. in: *Nanoelectronics and Information Technology*, *Advanced Electronic Materials and Novel Devices* (Waser, R., Ed.), pp 645-658, Wiley VCH, Weinheim, 2003.
[3] Wuttig M.: Nat. Mater. **4**, 265 (2005).
[4] Steimer C., Welnic W., Kalb J., Wuttig M.: J. Optoelectron. Adv. Mater. **8**, 2044 (2006).
[5] Borg H.J., van Woudenberg R.: J. Magn. Magn. Mater. **193**, 519 (1999).
[6] Zhou G.F.: Mater. Sci. Eng. A – Struct. Mater. Prop. Microstruct. Process. **304** (Spec. Iss.), 73 (2001).
[7] Purvis G.: III-Vs Review **19**, 39 (2006).
[8] Lacaita A. L.: Solid-State Electron. **50**, 24 (2006).
[9] Kozicki M.N., Mitkova M.: J. Non-Cryst. Solids **299-302 Part 2**, 1023 (2002).
[10] Kozicki M.N., Mitkova M., Park M., Balakrishnan M., Gopalan C.: Superlattices Microstruct. **34**, 459 (2003).
[11] Kozicki M.N., Mitkova M.: J. Non-Cryst. Solids **352**, 567 (2006).
[12] Ohta T.: J. Optoelectron. Adv. Mater. **3**, 609 (2001).
[13] Ohta T., Nishiuchi K., Narumi K., Kitaoka Y., Ishibashi H., Yamada N., Kozaki T.: Jpn. J. Appl. Phys. **39** (2B Part 1), 770 (2000).
[14] Hyot B., Poupinet L., Gehanno V., Desre P.J.: J. Magn. Magn. Mater. **249,** 504 (2002).
[15] Dieker H., Wuttig M.: Thin Solid Films **478**, 248 (2005).
[16] Li J., Hou L., Ruan H., Xie Q., Gan F.: Proc. SPIE **4085**, 125 (2001).
[17] Li J., Gan F.: Thin Solid Films **402**, 232 (2002).
[18] Welnic W., Pamungkas A., Detemple R., Steimer C., Blugel S., Wuttig M.: Nat. Mater. **5**, 56 (2006).
[19] Gan F.: J. Non-Cryst. Solids **256-257**, 176 (1999).
[20] Kolobov A.V., Fons P., Frenkel A.I., Ankudinov A.L., Tominaga J., Uruga T.: Nat. Mater. **3**, 703 (2004).
[21] Tashiro H., Harigaya M., Kageyama Y., Ito K., Shinotsuka M., Tani K., Watada A., Yiwata N., Nakata Y., Emura S.: Jpn. J. Appl. Phys. **41**, 3758 (2002).
[22] Kalb J., Spaepen F., Wuttig M.: J. Appl. Phys. **93**, 2389 (2003).
[23] Kolobov A.V., Fons P., Tominaga J., Uruga T.: J. Non-Cryst. Solids **352**, 1612 (2006).
[24] Paesler M.A., Baker D.A., Lucovsky G., Edwards A.E., Taylor P.C.: J. Optoelectron. Adv. Mater. **8**, 2039 (2006).

[25] Kolobov A.V., Haines J., Pradel A., Ribes M., Fons P., Tominaga J.: J. Optoelectron. Adv. Mater. **8**, 2161 (2006).
[26] Liu B., Song Z., Zhang T., Feng S., Chen B.: Appl. Surf. Sci. **242**, 62 (2005).
[27] Liu B., Song Z., Zhang T., Xia J., Feng S., Chen B.: Thin Solid Films **478**, 49 (2005).
[28] Lin S.S.: Ceram. Int. **33**, 1161 (2006).
[29] Gutwirth J., Wágner T., Kasap S.O., Frumar M.: J. Optoelectron. Adv. Mater. **7**, 1813 (2005).
[30] Gutwirth J., Wágner T., Bezdička P., Kotulánová E., Vlček Mil., Kasap S.O., Frumar M.: J. Non-Cryst. Solids **353**, 1431 (2007).
[31] Gutwirth J., Wágner T., Bezdička P., Vlček Mil., Kasap S.O., Frumar M.: J. Optoelectron. Adv. Mater. **9**, 3064 (2007).
[32] Gutwirth J., Wágner T., Němec P., Kasap S.O., Frumar M.: J. Non-Cryst. Solids **354**, 497 (2008).
[33] Mehta N., Zulfequar M., Kumar A., Phys. Status Solidi A – Appl. Mat. **203**, 236 (2006).
[34] Mehta N., Tiwari R.S., Kumar A.: Mat. Res. Bull. **41**, 1664 (2006).
[35] Babeva Tz., Dimitrov D., Kitova S., Konstantinov I.: Vacuum **58**, 496 (2000).
[36] Wang K., Steimer C., Detemple R., Wamwangi D., Wuttig M.: Appl. Phys A-Mater. Sci. Process. **81**, 601 (2005).
[37] Sharma Y.D., Bhatnagar R.K.: Opt. Eng. **41**, 1668 (2002).
[38] Xu J., Liu B., Song Z., Feng S., Chen B.: Mater. Sci. Eng. B-Solid State Mater. Adv. Technol. **127**, 228 (2006).
[39] Liu B., Song Z., Feng S., Chen B.: Microelectron. Eng. **82**, 168 (2005).
[40] Arun P., Vedeshwar A.G.: J. Appl. Phys., **79**, 4029 (1996).
[41] Arun P., Wedeshwar A.G.: J. Non-Cryst. Solids **220**, 63 (1997).
[42] Arun P., Vedeshwar A.G., Mehra N.C.: Mater. Res. Bull. **32**, 907 (1997).
[43] Arun P., Vedeshwar A.G., Mehra N.C.: J. Phys. D: Appl. Phys. **2**, 183 (1999).
[44] Wágner T., Macková A., Peřina V., Rauhala E., Seppälä A., Kasap S.O., Frumar M., Vlček Mir., Vlček Mil.: J. Non-Cryst. Solids **299-302 Part 2**, 1028 (2002).
[45] Frumar M., Wágner T.: Curr. Opin. Solid State Mat. Sci. **7**, 117 (2003).
[46] Swanepoel R.: J. phys. E: Sci. Instrum. **16**, 1214 (1983).
[47] JCPDS PDF-2 database, International Centre for Diffraction Data, Newtown Square, PA, U.S.A., release 54, (2004).